Molecular BioSystems

Dynamic Article Links

Cite this: *Mol. BioSyst.*, 2012, **8**, 3288–3294

www.rsc.org/molecularbiosystems

PAPER

Modification of calcium carbonate based gene and drug delivery systems by a cell-penetrating peptide

Dong Zhao, Ren-Xi Zhuo and Si-Xue Cheng*

Received 15th June 2012, Accepted 3rd October 2012
DOI: 10.1039/c2mb25233c

In this study, a facile strategy to effectively improve the gene and drug delivery efficiencies of calcium carbonate based nanoparticles was developed by introducing a cell-penetrating peptide, KALA, into the delivery systems. To evaluate the effect of KALA on the gene delivery efficiency, luciferase reporter gene plasmid was encapsulated in $CaCO_3$–KALA–DNA nanoparticles. The measurements of a Zetasizer showed that the size and the zeta potential of $CaCO_3$–KALA–DNA nanoparticles increased with increasing KALA amount because of the addition of positively charged KALA. Due to the existence of KALA, the gene expressions could be significantly enhanced in both HeLa and 293T cells. Confocal microscopy observation showed that the cellular uptake of $CaCO_3$–KALA–DNA nanoparticles was obviously enhanced compared to $CaCO_3$–DNA nanoparticles. To investigate the gene and drug co-delivery property, p53 expression plasmid and doxorubicin hydrochloride (DOX) were loaded in $CaCO_3$–KALA–p53–DOX nanoparticles. The *in vitro* cell growth inhibition effect of $CaCO_3$–KALA–p53–DOX nanoparticles was evaluated by MTT assay. Compared with $CaCO_3$–p53–DOX nanoparticles, $CaCO_3$–KALA–p53–DOX nanoparticles exhibited enhanced delivery efficiency, which led to a stronger inhibition effect on HeLa cells. These results indicated that the addition of KALA, which facilitated the cellular uptake of various agents, could improve both gene and drug delivery efficiencies. The KALA modified $CaCO_3$ based nanoparticles have promising applications in cancer treatments.

Introduction

In cancer treatments, existing clinical chemotherapy is still far from perfect because of drug resistance, low bioavailability and undesirable severe side effects. To overcome these limitations, drug delivery techniques with the aim to improve the therapeutic effect have been intensively investigated.[1] On the other hand, as one of the most promising approaches for cancer therapy, gene therapy has received increasing research interest.[2] For both drug delivery and gene delivery, efficient and safe delivery systems, which can deliver the therapeutic agents to particular tumor cells, are the key to improve the therapeutic effect.

To achieve more effective gene delivery, plenty of efforts have been made to modify delivery carriers by using functional peptides.[3–5] Among different peptides, cell-penetrating peptides (CPPs) with the ability to transport across plasma membranes, have been developed as delivery agents for various therapeutic agents.[6] KALA, a cationic endosomolytic and fusogenic peptide, can destabilize lipid membranes and facilitate cellular uptake of various membrane-impermeable agents. Besides being directly used as a gene vector to condense pDNA[7,8] and siRNA,[9] KALA and KALA derivatives such as PEG–KALA can also be incorporated into vector–DNA complexes as additives to achieve enhanced transfection efficiency.[10–14]

Compared to the widely investigated non-viral vectors based on cationic polymers and cationic liposomes, the technique of co-precipitation of Ca^{2+} with DNA in the presence of inorganic anions, such as CO_3^{2-} and PO_4^{3-}, has its unique advantages in terms of safety and biocompatibility.[15–21] In our previous study, we used KALA to modified nanostructured Ca–P to achieve enhanced gene delivery efficiency.[14] The *in vitro* study showed that the gene expression could be significantly enhanced with the addition of KALA for both solution-based transfection and substrate-mediated transfection.

In cancer treatments, considerable research interest has been focused on the combined drug and gene therapy with a synergistic therapeutic effect.[21–23] In current study, we investigated the effects of KALA modification on nano-structured $CaCO_3$ for the delivery of a reporter gene plasmid (pGL3–Luc), as well as the co-delivery of an antitumor gene plasmid (p53) and a chemotherapy drug (DOX). The *in vitro* study showed the presence of KALA resulted in improved efficiency for both gene and drug deliveries. The peptide

Key Laboratory of Biomedical Polymers of Ministry of Education, Department of Chemistry, Wuhan University, Wuhan 430072, P. R. China. E-mail: chengsixue@whu.edu.cn, chengsixue@hotmail.com; Fax: +86 27 6875 4509; Tel: +86 27 6875 4061

modified nanostructured $CaCO_3$ has promising applications in cancer treatments.

Results and discussion

KALA modified $CaCO_3$ based nanoparticles for gene delivery

In this study, a cationic endosomolytic and fusogenic peptide, KALA, was used to modify nanostructured $CaCO_3$ based gene delivery systems. Based on our previous study, the Ca^{2+}–CO_3^{2-} ratio of 50 was suitable to prepare the $CaCO_3$–DNA nanoparticles. So in the current study, we fixed the Ca^{2+}–CO_3^{2-} ratio at 50 to prepare the $CaCO_3$ based nanoparticles.

To identify the precise role of KALA, we studied the effect of the different methods of adding KALA in gene delivery systems on the gene delivery efficiency. From our experiments, we found that the presence of KALA could significantly improve the gene delivery efficiency. However, the enhancement in gene expression was strongly dependent on the method of adding KALA. As shown in Fig. 1, as compared with method (a) ($CaCO_3$–KALA–DNA nanoparticles were added to the transfection assay), the improvements of both method (b) (KALA was added to the transfection assay together with $CaCO_3$–DNA nanoparticles) and method (c) (KALA was added to the transfection assay together with $CaCO_3$–KALA–DNA nanoparticles) were not so significant. For method (a), the positively charged KALA could interact with negatively charged DNA during the preparation of the nanoparticles, and the well combination of KALA and DNA was favorable for the gene delivery. In contrast, for method (b), KALA added after the formation of $CaCO_3$–DNA nanoparticles was mainly deposited on the surface of the $CaCO_3$–DNA nanoparticles, which was not so effective to enhance the gene delivery efficiency. For method (c), KALA could not well interact with $CaCO_3$–KALA–DNA nanoparticles to deposit on the surface of the nanoparticles because both of them were positively charged and the excess KALA could not improve the gene delivery efficiency. Since adding KALA before the nanoparticle formation resulted in the highest enhancement of gene expression, KALA was added in the system before co-precipitation in this investigation unless otherwise mentioned.

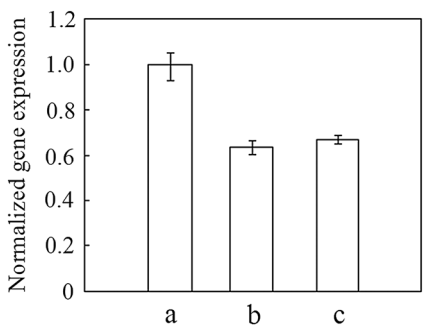

Fig. 1 Normalized gene expressions of different gene transfection methods. (a) $CaCO_3$–KALA–DNA nanoparticles containing 5 μg KALA was added to the transfection assay, (b) 5 μg KALA was added to the transfection assay together with $CaCO_3$–DNA nanoparticles, and (c) 5 μg KALA was added to the transfection assay together with $CaCO_3$–KALA–DNA nanoparticles containing 5 μg KALA. The data were normalized to the value of method (a).

The DNA encapsulation efficiencies of $CaCO_3$–DNA nanoparticles and $CaCO_3$–KALA–DNA nanoparticles with different KALA amounts are shown in Table 1. There were no obvious changes in DNA encapsulation efficiency for $CaCO_3$–KALA–DNA nanoparticles as compared to $CaCO_3$–DNA nanoparticles. All $CaCO_3$–KALA–DNA nanoparticles could achieve a high DNA encapsulation efficiency of about 90%. It can be concluded that the addition of KALA did not have influence on DNA encapsulation efficiency for the KALA amounts we used.

The sizes and zeta potential of $CaCO_3$–DNA nanoparticles and $CaCO_3$–KALA–DNA nanoparticles with different KALA amounts were measured by a Zetasizer. From Table 1, the sizes of all $CaCO_3$–KALA–DNA nanoparticles were larger than that of $CaCO_3$–DNA nanoparticles, and the size of $CaCO_3$–KALA–DNA nanoparticles increased with increasing KALA amount. As listed in Table 1, $CaCO_3$–DNA nanoparticles exhibited a slightly negative charge. With the addition of the cationic peptide, all $CaCO_3$–KALA–DNA nanoparticles showed positive charges, and the charge increased with increasing KALA amount. This result is reasonable if we compare the amounts of the positively charged KALA (1–10 μg) and negatively charged DNA (1 μg). In this study, to prepare the KALA containing nanoparticles, KALA was mixed with DNA in an aqueous medium and then $CaCl_2$ solution was immediately added. Thereafter $CaCO_3$–KALA–DNA nanoparticles were rapidly formed after the addition of Na_2CO_3 solution. During this process, KALA might not be well complexed with DNA, and the excess KALA might be present on the surface of the nanoparticles, which led to a positive zeta potential.

In this investigation, all the transfections were carried out in the complete medium (DMEM containing 10% FBS). As shown in Fig. 2, the gene expression mediated by all $CaCO_3$–KALA–DNA nanoparticles was higher than that mediated by $CaCO_3$–DNA nanoparticles in HeLa cells. Transfection efficiency of $CaCO_3$–KALA–DNA nanoparticles was strongly dependent on the KALA amount, *i.e.* the gene expression increased with increasing KALA amount and achieved a maximum value at the KALA amount of 5 μg and then decreased if the KALA amount was further increased to 10 μg. In addition, the maximum transfection efficiency of $CaCO_3$–KALA–DNA nanoparticles was much higher than that of commercially available transfection reagent Lipofectamine 2000 (LF). The gene expression results clearly indicated that the transfection efficiency of $CaCO_3$ based nanoparticles could be significantly enhanced with the modification of KALA peptide.

According to previous studies, KALA could interact with and destabilize lipid membranes, and thus facilitate the cellular entry by its ability to form an amphipathic α-helical structure. As a result, KALA could induce marked increase in transfection efficiency when being used as a component to form composite gene delivery systems with other polycation vectors.[7,8,24] In addition, it should be noted that, as compared with the $CaCO_3$–DNA nanoparticles, the increased zeta potential and particle size of $CaCO_3$–KALA–DNA nanoparticles could also affect their gene delivery efficiency. The positive zeta potential of the $CaCO_3$–KALA–DNA nanoparticles with a suitable amount of KALA, which was favorable for gene delivery, also played a role in the enhanced gene expression level.

Table 1 Properties of nanoparticles with different KALA amounts

Sample	KALA amount (μg)	Encapsulation efficiency of DNA (%)	Size (nm)	Zeta potential (mV)
$CaCO_3$–DNA	0	91.0 ± 0.8	198.4 ± 11.5	−0.98 ± 0.18
$CaCO_3$–KALA–DNA	1	89.7 ± 1.1	301.0 ± 12.3	1.75 ± 0.37
$CaCO_3$–KALA–DNA	2	90.2 ± 4.4	347.3 ± 10.0	3.96 ± 0.57
$CaCO_3$–KALA–DNA	5	89.6 ± 2.6	432.9 ± 24.2	20.95 ± 3.28
$CaCO_3$–KALA–DNA	10	88.6 ± 3.5	482.5 ± 27.8	28.95 ± 5.36

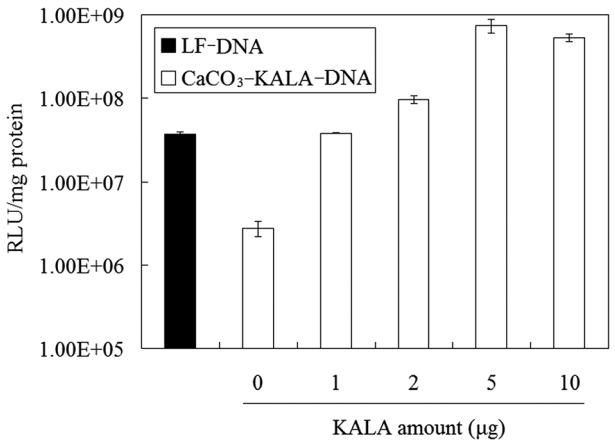

Fig. 2 Luciferase expression in HeLa cells after transfection for 48 h mediated by $CaCO_3$–KALA–DNA nanoparticles with different KALA amounts as compared with Lipofectamine 2000–DNA (LF–DNA).

Addition of excess KALA did not further increase the transfection activity. The possible reason is as follows. Excess KALA could not bind with DNA efficiently so that the improvement in gene expression through facilitating the cellular entry and endosomal escape could not be further improved.

To study the cellular uptake of $CaCO_3$–KALA–DNA nanoparticles, we used a confocal microscope to visualize the cells after being transfected for 4 h. As depicted in Fig. 3, green fluorescence dots could be observed inside the cells, indicating the internalization of YOYO-1 labeled pGL3-Luc. With an increase in the KALA amount, the green fluorescence dots increased obviously. The highest density of the green fluorescence dots was observed at the KALA amount of 5 μg. With a further increase in KALA amount, the density of green fluorescence dots decreased. This trend is in agreement with the gene expression result. From this observation, we can confirm that the addition of KALA peptide improved the transfection efficiency of $CaCO_3$ based nanoparticles by enhancing the cellular uptake.

Practical applications of a gene delivery system require a high level of gene expression as well as a low level of cytotoxicity. In the current study, we evaluated the *in vitro* cytotoxicity of the nanoparticles by MTT assay. From Fig. 4, it could be found that the cell viabilities were higher than 90% after being transfected by different nanoparticles for 48 h, implying that $CaCO_3$–KALA–DNA nanoparticles did not have apparent cytotoxicity. This result indicated that the presence of KALA did not lead to increased cytotoxicity.

In the present study, we also investigated the transfection efficiencies of the $CaCO_3$–KALA–DNA nanoparticles prepared with different KALA amounts in 293T cells. As shown in Fig. 5, for 293T cells, a similar trend was observed and the maximum

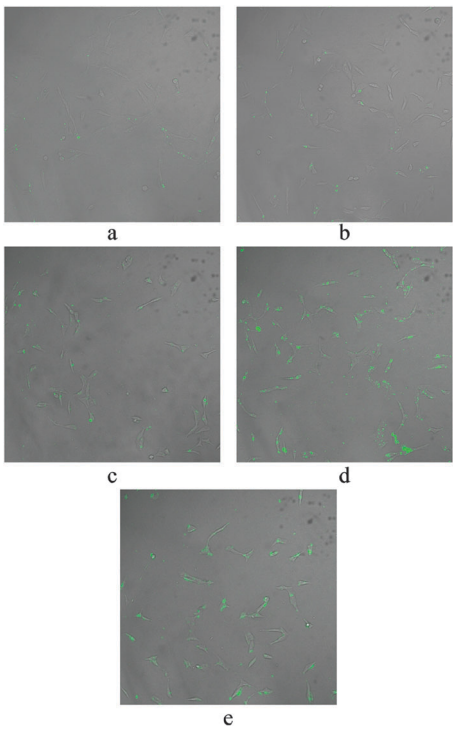

Fig. 3 Confocal images of HeLa cells after being treated by different $CaCO_3$–KALA–DNA nanoparticles with different KALA amounts for 4 h. (a) $CaCO_3$–DNA nanoparticles. (b)–(e) $CaCO_3$–KALA–DNA nanoparticles with different KALA amounts (1, 2, 5, and 10 μg, respectively).

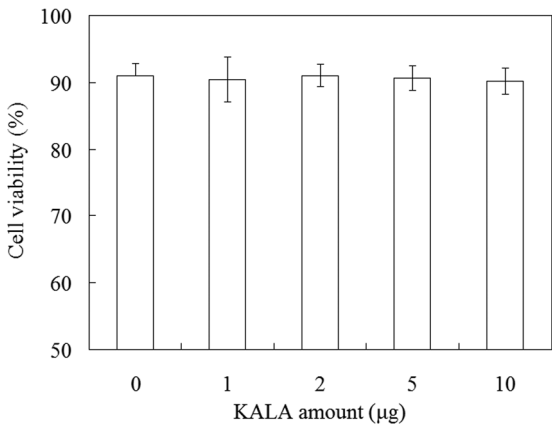

Fig. 4 Cell viability of HeLa cells after transfection for 48 h mediated by $CaCO_3$–KALA–DNA nanoparticles with different KALA amounts.

expression level was achieved at the KALA amount of 5 μg. Compared with HeLa cells, the luciferase expression levels for 293T cells were relatively high. The difference in expression

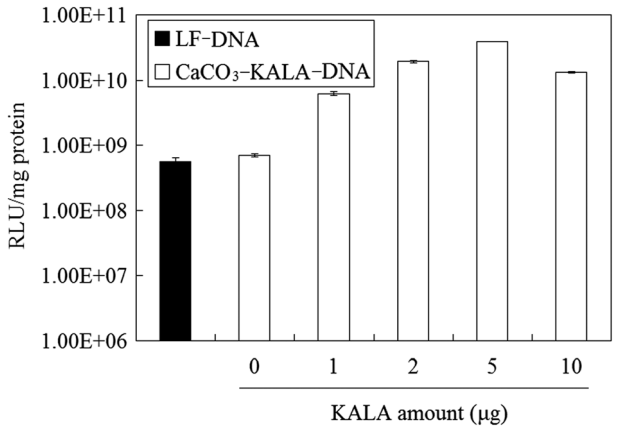

Fig. 5 Luciferase expression in 293T cells after transfection for 48 h mediated by $CaCO_3$–KALA–DNA nanoparticles with different KALA amounts as compared with Lipofectamine 2000–DNA (LF–DNA).

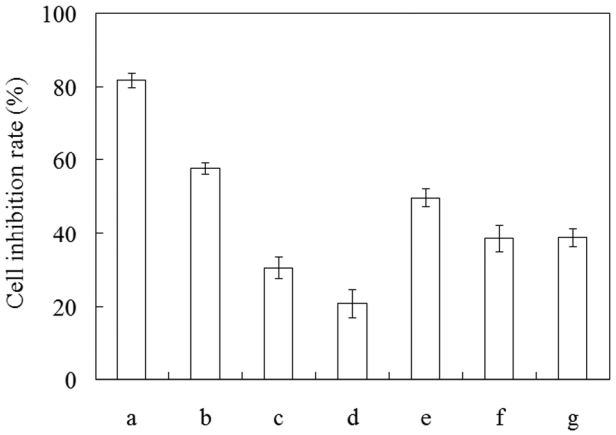

Fig. 6 Cell inhibition rate of HeLa cells after different treatments for 48 h. (a) $CaCO_3$–KALA–p53–DOX nanoparticles, (b) $CaCO_3$–p53–DOX nanoparticles, (c) $CaCO_3$–KALA–p53 nanoparticles, (d) $CaCO_3$–p53 nanoparticles, (e) $CaCO_3$–KALA–DNA–DOX nanoparticles loaded with the reporter gene plasmid pGL3-Luc, (f) $CaCO_3$–DNA–DOX nanoparticles loaded with the reporter gene plasmid pGL3-Luc, and (g) free DOX.

levels in different cells is a result of the specifications of the different cell lines. As it is well known, 293T cells are relatively easy to be transfected.

KALA modified $CaCO_3$ based nanoparticles for co-delivery of gene and drug

In the current investigation, gene and drug loaded $CaCO_3$–KALA–p53–DOX nanoparticles were prepared through a facile co-precipitation method, *i.e.* the nanoparticles were fabricated by mixing the solution containing KALA, p53 plasmid, DOX and Ca^{2+} ions with the solution containing CO_3^{2-} ions. For comparison, other types of nanoparticles loaded with the antitumor gene plasmid p53 or the reporter gene plasmid pGL3-Luc were also prepared. Since the KALA amount of 5 μg was suitable for improving the gene delivery efficiency, we used this fed amount to prepare KALA containing nanoparticles.

As listed in Table 2, the DOX encapsulation efficiencies of $CaCO_3$–KALA–p53–DOX nanoparticles and $CaCO_3$–p53–DOX nanoparticles were both higher than 80%, indicating that a co-precipitation technique could effectively encapsulate the water soluble drug (doxorubicin hydrochloride). The addition of positively charged KALA in the co-precipitation systems did not affect the encapsulation efficiencies of DOX.

Based on our experiments, the IC_{50} (half maximal inhibitory concentration) of free DOX was about 0.2 μg ml^{-1} for HeLa cells. So in the current study, we prepared DOX loaded nanoparticles with the DOX amount of 0.2 μg. To evaluate the gene and drug co-delivery efficiency of the nanoparticles, the cell growth inhibition effects were studied after the HeLa were treated by different nanoparticles. The results are summarized in Fig. 6. Compared with the treatments by p53 and DOX simultaneously, the treatments by p53 or DOX separately resulted in much lower cell inhibition rates. For example, the cell inhibition rates of $CaCO_3$–KALA–p53 nanoparticles, $CaCO_3$–p53 nanoparticles and free DOX were 30.4%, 20.8% and 38.7%, respectively, and the cell inhibition rates of $CaCO_3$–KALA–p53–DOX nanoparticles and $CaCO_3$–p53–DOX nanoparticles were 81.9% and 57.7%. Clearly, the inhibition effects of gene (p53) and drug (DOX) co-delivery systems were much better than that of the individual application of the gene or the drug.

Table 2 DOX loading properties of different nanoparticles

Sample	Encapsulation efficiency of DOX (%)	Loading content of DOX (wt%)
$CaCO_3$–KALA–p53–DOX	81.3	0.7
$CaCO_3$–p53–DOX	86.2	1.0

As shown in Fig. 6, the cell growth inhibition effect of $CaCO_3$–KALA–p53 nanoparticles was stronger than that of $CaCO_3$–p53 nanoparticles. This result was in accordance with the transfection results of the reporter gene plasmid, indicating KALA could improve p53 gene delivery efficiency.

In addition, the inhibition effect of $CaCO_3$–KALA–p53–DOX nanoparticles was much higher than that of $CaCO_3$–p53–DOX nanoparticles. As mentioned before, the addition of KALA in the delivery systems could enhance the cellular uptake. As a result, the KALA modification on the co-delivery system led to a significantly enhanced cell growth inhibition, implying that KALA could improve both gene and drug delivery efficiencies.

To study the precise role of each component, we also tried to fabricate $CaCO_3$ based nanoparticles loaded with DOX only. However, due to the absence of positively charged DNA, DOX loaded nanoparticles could not be formed with a controllable size. Thus, we prepared $CaCO_3$–KALA–DNA–DOX and $CaCO_3$–DNA–DOX nanoparticles loaded with the reporter gene plasmid pGL3-Luc and DOX. As mentioned before, the $CaCO_3$ based nanoparticles loaded with pGL3-Luc did not exhibit apparent cytotoxicity. Thus, we can assume that the cell growth inhibition of $CaCO_3$–KALA–DNA–DOX and $CaCO_3$–DNA–DOX nanoparticles was mainly caused by the DOX component. As demonstrated in Fig. 6, compared with free DOX, $CaCO_3$–DNA–DOX nanoparticles had a similar cell inhibition growth effect. With the addition of KALA, $CaCO_3$–KALA–DNA–DOX nanoparticles exhibited an enhanced cell

inhibition rate. In addition, through comparing the inhibition effects of $CaCO_3$–KALA–p53–DOX and $CaCO_3$–KALA–DNA–DOX nanoparticles, we can find $CaCO_3$–KALA–p53–DOX nanoparticles possessed higher inhibition effect, which was due to the presence of p53.

The mechanism of cell growth inhibition of $CaCO_3$–KALA–p53–DOX nanoparticles was studied by using the FITC Annexin V/Dead Cell Apoptosis Kit. As we know, phosphatidylserine (PS) is only located on the cytoplasmic surface of the cell membrane for normal live cells. In the initial cell apoptosis period, PS is translocated from the inner to the outer leaflet of the cell membrane and this change is earlier than compaction and fragmentation of the nuclear chromatin, shrinkage of the cytoplasm, and loss of membrane asymmetry. The human anticoagulant, annexin V, is a Ca^{2+}-dependent phospholipid-binding protein that has a high affinity for PS. FITC Annexin V can identify apoptotic cells by binding to PS exposed on the outer leaflet. The red-fluorescent propidium iodide nucleic acid binding dye (PI) is impermeant to live cells and apoptotic cells, but stains the nuclei of dead cells with red fluorescence through binding to the nucleic acids in the cells. After staining a cell population with FITC annexin V and PI, apoptotic cells show green fluorescence, dead cells show red and green fluorescence, and live cells show little or no fluorescence under a confocal laser scanning microscope. Based on the evaluation by the FITC Annexin V/Dead Cell Apoptosis Kit, the living cells, dead cells, and cell apoptosis could be identified.

In this study, we stained HeLa cells with FITC annexin V and PI after the treatment by $CaCO_3$–KALA–p53–DOX nanoparticles for 48 h. As shown in Fig. 7, after the treatment for 48 h, most HeLa cells shrank and became rounded and strong red and green fluorescence could be clearly detected, indicating the cell death was mainly induced by apoptosis.

Experimental

Materials

Lipofectamine 2000 was purchased from Invitrogen. Anhydrous calcium chloride and anhydrous sodium carbonate of analytical grade were supplied by Sinopharm Chemical Reagent Co. Ltd. (Shanghai, China) and used as received. KALA peptide (WEAKLAKALAKALAKHLAKALAKALKACEA) with M_w = 3131 g mol^{-1} was obtained from GL Biochem (Shanghai, China). 3-(4,5-Dimethylthiazol-2-yl)-2,5-diphenyltetrazolium bromide (MTT) was from Amresco. Dimethylsulfoxide (DMSO) was from Sigma. Doxorubicin hydrochloride (DOX) was provided by Zhejiang Hisun Pharmaceutical Co. Ltd. (China).

Human embryonic kidney cell line 293T and human cervical carcinoma cell line HeLa were obtained from China Center for Typical Culture Collection (Wuhan, China). The medium for cell culture was Dulbecco's Modified Eagle's Medium (DMEM) (Gibco) supplemented with 10% fetal bovine serum (FBS), 2 mg ml^{-1} $NaHCO_3$, and 100 U ml^{-1} penicillin/streptomycin. Cells were incubated at 37 °C in humidified air/5% CO_2.

Luciferase plasmid (pGL3-Luc) and human wild-type p53 expression plasmids (p53) were amplified in *Escherichia coli* and extracted and purified by the QIAfilter Plasmid Mega Kit (QIAGEN). Plasmids were suspended in water and stored at −20 °C.

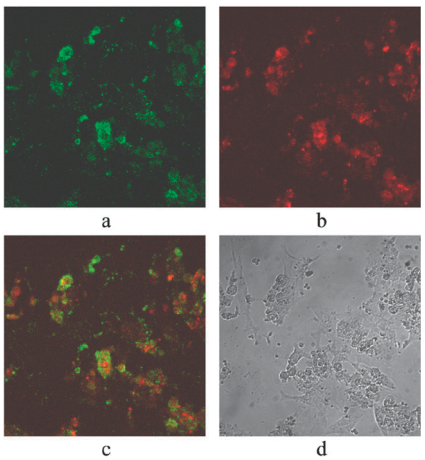

Fig. 7 Confocal images of HeLa cells after being treated by $CaCO_3$–KALA–p53–DOX nanoparticles for 48 h. (a) Green fluorescence image, (b) red fluorescence image, (c) overlapped images of red and green fluorescences, and (d) DIC images. The images were obtained under the magnification of 400.

Preparation and characterizations of $CaCO_3$–KALA–DNA nanoparticles

KALA solution (1 μg μl^{-1}) containing a particular amount of KALA (1, 2, 5 and 10 μg, respectively) was added to 1 μl of DNA solution containing 1 μg of pGL3-Luc, and then 16 μl of $CaCl_2$ solution (0.5 M), was immediately added. The mixture was diluted with deionized water to make solution **A** with a total volume of 50 μl. 16 μl of Na_2CO_3 solution (0.01 M) was diluted with deionized water to make solution **B** with a total volume of 50 μl. Solution **A** was rapidly added into solution **B** under stirring to obtain $CaCO_3$–KALA–DNA nanoparticles. The solution containing $CaCO_3$–KALA–DNA nanoparticles was immediately used for gene transfection.

For comparison, $CaCO_3$–DNA nanoparticles were prepared in the absence of KALA. Other conditions were the same as that for the preparation of $CaCO_3$–KALA–DNA nanoparticles.

The size and zeta potential of the nanoparticles were measured by a Zetasizer Nano ZS (Malvern Instruments). Prior to measurements, 800 μl deionized water was added to 200 μl of the freshly prepared nanoparticles containing solution (containing 2 μg of pGL3-Luc) for dilution. Data were given as mean ± standard deviation (SD) based on 3 independent measurements.

500 μl of $CaCO_3$–KALA–DNA nanoparticles containing solution was prepared as mentioned before and centrifuged at 4 °C for 1 h at 18 000 rpm. After centrifugation, the amount of non-precipitated free DNA remaining in the supernatant of solution was determined by the Quant-iT™ PicoGreen® dsDNA Assay Kit (Molecular Probes) according to the manufacturer's protocol using a spectrofluorophotometer (RF-5301 PC, Shimadzu). Data were given as mean ± standard deviation (SD) based on 3 independent measurements. The encapsulation efficiency of DNA was calculated as follows.

$$\text{Encapsulation efficiency} = (W_T - W_F)/W_T \times 100\%$$

where W_T is the total weight of DNA fed, and W_F is the weight of non-encapsulated free DNA.

In vitro transfection mediated by $CaCO_3$–KALA–DNA nanoparticles

The cells in 1 ml of complete medium (DMEM containing 10% FBS) were seeded directly in the well of a 24-well plate (5×10^4 cells per well) and incubated for 24 h. Then the solution (100 μl with 1 μg pGL3-Luc) containing freshly prepared $CaCO_3$–KALA–DNA nanoparticles was added to each well, and the cells were incubated at 37 °C. The gene expression was evaluated after 48 h.

To assay the expression of luciferase, the medium was removed and the cells were rinsed gently by phosphate buffered saline (PBS, 0.1 M, pH 7.4). After thorough lysis of the cells with reporter lysis buffer (Promega) (200 μl per well), the luciferase activity was determined by detecting the light emission from 20 μl cell lysate incubated with 100 μl of luciferin substrate (Promega) in a luminometer (Lumat LB9507, Berthold). The protein content of the cell lysate was determined by the BCA protein assay kit (Pierce). The optical density (OD) value was determined at 570 nm using a microplate reader (Bio-rad 550). The data were given as mean ± standard deviation (SD) based on 3 independent measurements.

For comparison, the expression of luciferase mediated by Lipofectamine 2000–DNA complexes was measured. To prepare the Lipofectamine 2000–DNA complexes, a Lipofectamine 2000 solution (1 μl in 50 μl deionized water) was added to a plasmid DNA solution (1 μg in 50 μl deionized water) and mixed gently. Then the mixture was incubated at room temperature for 30 min to obtain Lipofectamine 2000–DNA complexes.

Study on cellular uptake of $CaCO_3$–KALA–DNA nanoparticles

1 μg of pGL3-Luc was mixed with 2.5 μl of YOYO-1 water stock solution (10 μM) and incubated for 15 min at 37 °C. Then the YOYO-1 labeled pGL3-Luc was used to prepare $CaCO_3$–KALA–DNA nanoparticles and $CaCO_3$–DNA nanoparticles.

HeLa cells in complete medium (DMEM containing 10% FBS) were seeded directly in the well of a 24-well plate (5×10^4 cells per well). After incubation at 37 °C for 24 h, the nanoparticles containing solution (100 μl containing 1 μg YOYO-1 labeled pGL3-Luc) were added. After incubation for 4 h at 37 °C, the medium was removed and the cells were washed twice with PBS to remove the nanoparticles and free YOYO-1 staying outside the cells. Then 1 ml of complete medium was added. The cells were observed under excitation at 488 nm using a confocal laser scanning microscope (Nikon C1-si TE2000) under the magnification of 200. All confocal images were slice images to distinguish YOYO-1 labeled pGL3-Luc, internalized the cells, from that adhered to the outside of the cellular membranes.

Evaluation of cytotoxicity of $CaCO_3$–KALA–DNA nanoparticles

After the HeLa cells were treated by the nanoparticles for 48 h, the medium was removed, and then fresh medium (1 ml) and (3-(4,5-dimethylthiazol-2-yl)-2,5-diphenyltetrazolium bromide) (MTT) (60 μl, 5 mg ml^{-1}) were added to each well, followed by incubation at 37 °C for 4 h. Then the supernatant was carefully removed, and 1 ml DMSO was added to each well to dissolve the formazan crystals produced by viable cells. The absorbance of the solution was measured using a microplate reader (Bio-Rad 550) at 570 nm to determine the OD value. The data were given as mean ± standard deviation (SD) based on 3 independent measurements.

Preparation of $CaCO_3$–KALA–p53–DOX nanoparticles

KALA solution (1 μg μl^{-1}) containing 5 μg of KALA was added to 1 μl of DNA solution containing 1 μg of p53, and then the solution containing 0.2 μg of DOX and 16 μl of $CaCl_2$ solution (0.5 M) was immediately added. The mixture was diluted with deionized water to make solution **C** with a total volume of 50 μl. 16 μl of Na_2CO_3 solution (0.01 M) was diluted with deionized water to make solution **D** with a total volume of 50 μl. Solution **C** was rapidly added into solution **D** under stirring to obtain $CaCO_3$–KALA–p53–DOX by rapidly adding solution **C** into solution **D** under stirring. The solution containing $CaCO_3$–KALA–p53–DOX nanoparticles was immediately used for gene transfection.

For comparison, $CaCO_3$–p53–DOX, $CaCO_3$–KALA–p53 and $CaCO_3$–p53 nanoparticles were prepared in the absence of particular agents. $CaCO_3$–KALA–DNA–DOX and $CaCO_3$–DNA–DOX nanoparticles were prepared by using the reporter gene plasmid pGL3-Luc. Other conditions were similar to the preparation of $CaCO_3$–KALA–p53–DOX nanoparticles.

Evaluation of *in vitro* cell growth inhibition of different nanoparticles

HeLa cells in 1 ml of complete medium (DMEM containing 10% FBS) were seeded directly in the well of a 24-well plate (5×10^4 cells per well) and incubated at 37 °C for 24 h. Then the freshly prepared solution containing particular agents ($CaCO_3$–KALA–p53–DOX, $CaCO_3$–p53–DOX, $CaCO_3$–KALA–p53, $CaCO_3$–p53, $CaCO_3$–KALA–DNA–DOX, $CaCO_3$–DNA–DOX and free DOX, respectively) was added to each well, and the cells were incubated at 37 °C for 48 h. Then the cell inhibition rate was determined by MTT assay as follows. After the medium containing co-precipitates was removed, 1 ml of complete medium and (3-(4,5-dimethylthiazol-2-yl)-2,5-diphenyltetrazolium bromide) (MTT) (60 μl, 5 mg ml^{-1}) were added to each well, followed by incubation at 37 °C for 4 h. Then the supernatant was carefully removed, and 1 ml DMSO was added to each well to dissolve the formazan crystals produced by viable cells. The absorbance of the solution was measured using a microplate reader (Bio-Rad 550) at 570 nm to determine the OD value. The data were given as mean ± standard deviation (SD) based on 3 independent measurements. The cell inhibition rate was calculated as follows.

$$\text{Cell inhibition rate} = (1 - OD_{treated}/OD_{control}) \times 100\%$$

where $OD_{treated}$ was obtained from the cells treated by a particular agent, and $OD_{control}$ was obtained from the cells without any treatments.

Determination of encapsulation efficiency and loading content of DOX

2000 μl of nanoparticles containing solution (containing 20 μg of p53 and 4 μg of DOX) was prepared as mentioned before and centrifuged at 4 °C for 1 h at 18 000 rpm. After centrifugation, the amount of free DOX remaining in the supernatant

of solution was determined by the absorbance at 485 nm using a UV-vis spectrophotometer (PerkinElmer Lambda Bio 40). The encapsulation efficiency and loading content of DOX were calculated as follows.

$$\text{Loading content} = (W_T - W_F)/W_{NP} \times 100\%$$

where W_T is the total weight of DOX fed, W_F is the weight of non-encapsulated free DOX, and W_{NP} is the weight of nanoparticles.

$$\text{Encapsulation efficiency} = (W_T - W_F)/W_T \times 100\%$$

where W_T is the total weight of DOX fed, and W_F is the weight of non-encapsulated free DOX.

Apoptosis assay

The cell apoptosis was assayed by the FITC Annexin V/Dead Cell Apoptosis Kit with FITC annexin V and PI (Invitrogen). HeLa cells exposed to $CaCO_3$–KALA–p53–DOX nanoparticles containing solution for 48 h were washed with cold PBS and 1× annexin-binding buffer. Then 100 μl of 1× annexin-binding buffer, 5 μl of the annexin V conjugate (Component A) and 1 μl of the PI working solution (100 μg ml^{-1}) were added to the cells. After incubation for 15 min, the cells were washed with 1× annexin-binding buffer and observed using a confocal laser scanning microscope (Nikon C1-si TE2000) with excitation at 488 nm under the magnification of 400.

Conclusions

To enhance the delivery efficiency, KALA peptide was used to modify the nanostructured calcium carbonate based gene and drug delivery systems. The KALA peptide modification resulted in an enhanced cellular uptake of the nanoparticles. The gene delivery efficiency was strongly depended on the KALA amount. With an appropriate amount of KALA, the gene transfection efficiency of $CaCO_3$–KALA–DNA nanoparticles could be significantly improved. The cell growth inhibition study on the $CaCO_3$–KALA–p53–DOX anti-tumor gene and drug co-delivery system showed that the KALA modification could enhance the delivery efficiencies of gene and drug simultaneously to achieve an improved cell growth inhibition effect.

Acknowledgements

Financial support from National Natural Science Foundation of China (21074099 and 21274113), Ministry of Science and Technology of China (National Basic Research Program of China 2011CB606202), and Ministry of Education of China (Program for Changjiang Scholars and Innovative Research Team in University IRT1030) is gratefully acknowledged.

References

1 J. Shi, A. R. Votruba, O. C. Farokhzad and R. Langer, *Nano Lett.*, 2010, **10**, 3223–3230.
2 M. L. Edelstein, M. R. Abedi and J. Wixon, *J. Gene Med.*, 2007, **9**, 833–842.
3 K. S. Rao, M. K. Reddy, J. L. Horning and V. Labhasetwar, *Biomaterials*, 2008, **29**, 4429–4438.
4 N. Schmidt, A. Mishra, G. H. Lai and G. C. Wong, *FEBS Lett.*, 2010, **584**, 1806–1813.
5 Q. Y. Liang, L. H. Lai, J. Shen, Q. Q. Wang, F. J. Xu and G. P. Tang, *Biomaterials*, 2011, **32**, 7253–7263.
6 A. Bolhassani, *Biochim. Biophys. Acta, Rev. Cancer*, 2011, **1816**, 232–246.
7 J. Fominaya, M. Gasset, R. García, F. Roncal, J. P. Albar and A. Bernad, *J. Gene Med.*, 2000, **2**, 455–464.
8 K. Rittner, A. Benavente, A. Bompard-Sorlet, F. Heitz, G. Divita, R. Brasseur and E. Jacobs, *Mol. Ther.*, 2002, **5**, 104–114.
9 J. Kim, S. H. Lee, J. Choe and T. G. Park, *J. Gene Med.*, 2009, **11**, 804–812.
10 S. H. Min, D. C. Lee, M. J. Lim, H. S. Park, D. M. Kim, C. W. Cho, D. Y. Yoon and Y. I. Yeom, *J. Gene Med.*, 2006, **8**, 1425–1434.
11 H. Lee, J. H. Jeong and T. G. Park, *J. Controlled Release*, 2001, **76**, 183–192.
12 H. Lee, J. H. Jeong and T. G. Park, *J. Controlled Release*, 2002, **79**, 283–291.
13 D. W. Lim, Y. I. Yeom and T. G. Park, *Bioconjugate Chem.*, 2000, **11**, 688–695.
14 S. Chen, R. X. Zhuo and S. X. Cheng, *J. Gene Med.*, 2010, **12**, 705–713.
15 E. H. Chowdhury, T. Sasagawa, M. Nagaoka, A. K. Kundu and T. Akaike, *Anal. Biochem.*, 2003, **314**, 316–318.
16 D. Olton, J. Li, M. E. Wilson, T. Rogers, J. Close, L. Huang, P. N. Kumta and C. Sfeir, *Biomaterials*, 2007, **28**, 1267–1279.
17 A. Hanifi, M. H. Fathi and H. Mir Mohammad Sadeghi, *J. Mater. Sci. Mater. Med.*, 2010, **21**, 2601–2609.
18 B. Sun, K. K. Tran and H. Shen, *Biomaterials*, 2009, **30**, 6386–6393.
19 E. H. Chowdhury, A. Maruyama, A. Kano, M. Nagaoka, M. Kotaka, S. Hirose, M. Kunou and T. Akaike, *Gene*, 2006, **376**, 87–94.
20 T. Y. Cheang, S. M. Wang, Z. J. Hu, Z. H. Xing, G. Q. Chang, C. Yao, Y. Liu, H. Zhang and A. W. Xu, *J. Mater. Chem.*, 2010, **20**, 8050–8055.
21 S. Chen, D. Zhao, F. Li, R. X. Zhuo and S. X. Cheng, *RSC Adv.*, 2012, **2**, 1820–1826.
22 N. Wiradharma, Y. W. Tong and Y. Y. Yang, *Biomaterials*, 2009, **30**, 3100–3109.
23 X. Lu, Q. Q. Wang, F. J. Xu, G. P. Tang and W. T. Yang, *Biomaterials*, 2011, **32**, 4849–4856.
24 T. B. Wyman, F. Nicol, O. Zelphati, P. V. Scaria, C. Plank and F. C. Szoka, *Biochemistry*, 1997, **36**, 3008–3017.

